



H₂S Protects Against Immobilization-Induced Muscle Atrophy via Reducing Oxidative Stress and Inflammation

Miaomiao Xu¹, Xiaoguang Liu², Peng Bao¹, Yan Jie Wang¹, Jianqiang Lu^{1*} and Yu Jian Liu^{1*}

¹School of Kinesiology, Shanghai University of Sport, Shanghai, China, ²Guangzhou Sport University Sports and Health, Guangzhou Sport University, Guangzhou, China

OPEN ACCESS

Edited by:

Jianjie Ma,
The Ohio State University,
United States

Reviewed by:

Anand Thirupathi,
Ningbo University, China
Chuanxi Cai,
The Ohio State University,
United States

*Correspondence:

Jianqiang Lu
lujianqiang@sus.edu.cn
Yu Jian Liu
liuyujian@sus.edu.cn

Specialty section:

This article was submitted to
Striated Muscle Physiology,
a section of the journal
Frontiers in Physiology

Received: 29 December 2021

Accepted: 24 March 2022

Published: 06 April 2022

Citation:

Xu M, Liu X, Bao P, Wang YJ, Lu J and
Liu YJ (2022) H₂S Protects Against
Immobilization-Induced Muscle
Atrophy via Reducing Oxidative Stress
and Inflammation.
Front. Physiol. 13:844539.
doi: 10.3389/fphys.2022.844539

Chronic inflammation and oxidative stress are major triggers of the imbalance between protein synthesis and degradation during the pathogenesis of immobilization-induced muscle atrophy. This study aimed to elucidate the effects of hydrogen sulfide (H₂S), a gas transmitter with potent anti-inflammatory and antioxidant properties, on immobilization-induced muscle atrophy. Mice were allocated to control and immobilization (IM) groups, which were treated with slow (GYY4137) or rapid (NaHS) H₂S releasing donors for 14 days. The results showed that both GYY4137 and NaHS treatment reduced the IM-induced muscle loss, and increased muscle mass. The IM-induced expressions of Muscle RING finger 1 (MuRF1) and atrogin-1, two muscle-specific E3 ubiquitin ligases, were decreased by administration of GYY4137 or NaHS. Both GYY4137 and NaHS treatments alleviated the IM-induced muscle fibrosis, as evidenced by decreases in collagen deposition and levels of tissue fibrosis biomarkers. Moreover, administration of GYY4137 or NaHS alleviated the IM-induced infiltration of CD45⁺ leukocytes, meanwhile inhibited the expressions of the pro-inflammatory biomarkers in skeletal muscles. It was found that administration of either GYY4137 or NaHS significantly attenuated immobilization-induced oxidative stress as indicated by decreased H₂O₂ levels and 8-hydroxy-2'-deoxyguanosine (8-OHdG) immunoreactivity, as well as increased total antioxidant capacity (T-AOC), nuclear factor erythroid-2-related factor 2 (NRF2) and NRF2 downstream anti-oxidant targets levels in skeletal muscles. Collectively, the present study demonstrated that treatment with either slow or rapid H₂S releasing donors protected mice against immobilization-induced muscle fibrosis and atrophy. The beneficial effects of H₂S on immobilization-induced skeletal muscle atrophy might be due to both the anti-inflammatory and anti-oxidant properties of H₂S.

Keywords: H₂S, immobilization, muscle atrophy, fibrosis, inflammation, oxidative stress

INTRODUCTION

Long-term bed rest or unloading leads to muscle atrophy, which is associated with substantial prevalence and financial burden all over the world (Edwards et al., 2015). Muscle atrophy occurs when protein degradation rates exceed protein synthesis (Wall et al., 2013b). Two major protein degradation pathways, the proteasomal and the autophagic-lysosomal pathways, are activated during

muscle atrophy. Growing evidence has shown that immobilization-induced muscle atrophy is a chronic inflammatory reaction (Komatsu et al., 2018), which is characterized by increases of pro-inflammatory biomarkers (Caron et al., 2011). Subsequently, the pro-inflammatory cytokines, such as TNF- α and IL-6, promote the muscle atrophy process by activating the ubiquitin-proteasome system, ultimately leading to muscle loss and functional impairment (Sente et al., 2016).

On the other hand, oxidative stress is recently considered as another major trigger of the imbalance between protein synthesis and degradation during the pathogenesis of immobilization-induced muscle atrophy (Pellegrino et al., 2011). Elevated production of ROS in disused skeletal muscles is found to activate both ubiquitin-proteasomal and the autophagolysosomal pathways, thus promoting muscle atrophy (Shenton et al., 2006). Notably, excessive ROS is also found to induce muscle atrophy through activating NF- κ B pro-inflammatory signaling pathway (Zhao S et al., 2020). Taken together, these studies suggest that anti-inflammatory agents and/or antioxidants may be useful for the treatment of immobilization-induced muscle atrophy.

H₂S, as a gas transmitter, is found to regulate inflammatory responses and oxidative/redox signaling pathways in a variety of tissues including different types of muscles (Chen et al., 2021). As shown in the literature, H₂S donors exert complex and, at times, opposing effects such as pro-inflammatory or anti-inflammatory, pro-oxidant or anti-oxidant, cytotoxic or cytoprotective effects. One possible explanation for these discrepant data may be the different releasing patterns of H₂S donors used in these various studies. To the best of our knowledge, the effects of H₂S donors on immobilization-induced muscle atrophy remained unknown. Thus, the present study aimed to investigate and compare the effects of slow (GY4137) and rapid (NaHS) H₂S releasing donors on a mouse model of muscle atrophy induced by bilateral hindlimb immobilization. Our data showed that both slow and rapid H₂S releasing donors protected against immobilization-induced muscle atrophy and fibrosis via reducing inflammation and oxidative stress.

METHODS

Animals

Ten-week-old C57BL/6J male mice were obtained from the Model Animal Research Center of Nanjing University. Animals were housed in cages and given access to food and water ad libitum at a constant ambient temperature and humidity with 12 h day-night cycling. The experimental protocols were approved by the Ethics Review Committee for Animal Experimentation of the Shanghai University of Sport (102772020DW008).

Immobilization-Induced Muscle Atrophy Model and Hydrogen Sulfide Donors Administration

We used an experimental model of immobilization-induced muscle atrophy. Briefly, mice were anesthetized via

intraperitoneal injection of 35 mg/kg phenobarbital sodium. Both hindlimbs were shaved and wrapped in medical plaster with the knee extended, and the ankle positioned in plantar flexion to induce maximal atrophy of the both hindlimbs muscles (Frimel et al., 2005).

To evaluate the effect of slow H₂S releasing donor GYY4137 on immobilization-induced muscle atrophy, mice were randomly divided into three groups: 1) Control group; 2) Immobilization group; 3) Immobilization + GYY4137 group. Mice in immobilization + GYY group were injected intraperitoneally with GYY4137 (Sigma, United States) at 50 mg/kg once daily for 2 weeks. The control and immobilization groups received identical doses of saline once daily for 2 weeks.

To evaluate the effect of rapid H₂S releasing donor NaHS on immobilization-induced muscle atrophy, mice were randomly divided into three groups: 1) Control group; 2) Immobilization group; 3) Immobilization + NaHS group. Mice in immobilization + NaHS group were injected intraperitoneally with NaHS (Sigma, United States) at 1.12 mg/kg (20 μ mol/kg) twice a day for 2 weeks. The control and immobilization groups received identical doses of saline twice a day for 2 weeks.

The chosen doses of GYY4137 (Huang et al., 2021) and NaHS (Smink et al., 2020) were based on previous studies and our preliminary experiments showing that GYY4137 and NaHS at the doses of 50 mg/kg and 20 μ mol/kg were well tolerated in mice and significantly attenuated immobilization-induced muscle atrophy. Especially, in our preliminary experiments it was determined that the NaHS at the dose of 20 μ mol/kg had a better protective effect than 50 μ mol/kg in maintaining muscle mass and decreasing muscle atrophy related genes expressions (**Supplementary Figure S1**).

Histological Stainings

Tibialis anterior (TA) muscle tissues were fixed with 4% paraformaldehyde overnight. The fixed tissue samples were then embedded in paraffin. Serial transverse sections of muscle tissues with 5 μ m thickness were subjected to haematoxylin-eosin (HE) staining using commercial kit (KeyGEN, China) according to the instructions. Masson Trichromatic staining was performed with a Masson staining kit (Solarbio, China) according to the instructions.

Quantitative Real-Time PCR

Briefly, total RNA samples were extracted from the TA muscle tissues using TRIzol (Invitrogen, United States). RNA samples were then reverse-transcribed into cDNA using a kit from Thermo Scientific (Applied Biosystems, United States). Relative expression levels of RNA transcripts were determined using gene-specific primers (Sangon Biotech, China), SYBR green (Vazyme Biotech, Nanjing, China). The expression of genes was normalized to β -actin and analyzed by the 2- $\Delta\Delta$ CT method. Gene-specific primers were listed in **Table 1**.

Measurements of Total Antioxidant Capacity and H₂O₂

The total antioxidant capacity (T-AOC) and H₂O₂ content in the gastrocnemius (GAS) muscle tissue homogenates were detected

TABLE 1 | Primers for real-time RT-PCR.

Target gene	Forward primer sequences	Reverse primer sequences
Col1a1	5'-TGGTCCTGCTGGTCTGCTG-3'	5'-CTGTACCTTGTTCGCCTGTCTC-3'
Col1a2	5'-AGGTGGCAAAGTGAACAAGGC-3'	5'-GACCAGCAGGACCAGGGAGAC-3'
Col5a1	5'-CGAAGTTCTCAGCCGAGTG-3'	5'-GTCATAGGCAGCTCGTTGTGAC-3'
Col14a1	5'-CAGGCGTCAGGCTTCAGTGATG-3'	5'-GTAGGCTGTGGCATGGCGATG-3'
PDGFRa	5'-CAGGCAGGGCTTCAACGGAAC-3'	5'-GCGTGCCTCCATCTCCAGATTC-3'
TGF-β	5'-TTCCTGGCGTTACCT TGGT-3'	5'-CCACTGCCG GACAAC-3'
α-SMA	5'-GGCTTCGCTGGTGATGCTC-3'	5'-TCCCTCTCTTGGCTTTC-3'
IL-1β	5'-TGACGTTCCATTAGACAAC-3'	5'-CCGTCCTTTCATTACACAGGACA-3'
IL-6	5'-GAACAACGATGATGCACCTTGC-3'	5'-CTTCATGTAATCCAGGTAGCTATGGT-3'
TNF-α	5'-CCTGTAGCCACGTCGTAG-3'	5'-GGGAGTAGACAAGGTACAACCC-3'
NLRP3	5'-CGTTGCAAGCTGGCTCAGTA-3'	5'-GGGGACTGGGATACAGCCTT-3'
CCL2	5'-GCTCAGCCAGATGCAGTTAAC-3'	5'-CTCTCTCTTGGCTTGGTGAC-3'
MuRF-1	5'-ATCACGCAGGAGCAGGAGGAG-3'	5'-CTTGGCCTTGGAGAGGAGGTAGC-3'
Atrogin-1	5'-GTCGGCAAGTCTGTGCTGGT-3'	5'-AGGCAGGTGGGTGATCGTGAG-3'
NRF2	5'-TCTCCTCGCTGGAAAAGAA-3'	5'-AATGTCTGGCTGTGCTTTA-3'
HO-1	5'-TCTGGAATGGAGGGAGATACC-3'	5'-CAGCAGTCGTGGTCAGTCAA-3'
NQO1	5'-GCCAATCAGCGTTCCGGTAT-3'	5'-CCTCCCCTCTCTCTTCTTCA-3'
MRP5	5'-TGGGGGACTATGCCGCTAT-3'	5'-AGAAATTCTGCACCCAGCC-3'
ARK1B10	5'-ACCCGCTCCTACTGACTCCT-3'	5'-ACATTGCCCTTGTGCTGAGAT-3'
β-actin	5'-TGGAAGGTGGACAGTGAGGC-3'	5'-CCAGGCATTGCTGACAGG-3'

according to the manufacturer's instructions (Westang, Shanghai, China). All results were standardized by the protein concentration of muscle homogenates.

Immunofluorescence

Paraffin sections (4 μm) of TA muscle tissues were rehydrated and microwaved in citric acid buffer to retrieve antigens. After incubation with 10% BSA for 1 h, the sections were respectively incubated with primary antibodies against CD45 (1:200; Abcam, MA, United States) and 8-hydroxy-2'-deoxyguanosine (8-OHdG) (1:200; Abcam) overnight. Subsequently, tissue slices were incubated with secondary antibody corresponding to each primary antibodies in dark for 1 h and counter-stained with 4',6-diamidino-2-phenylindole (DAPI) (Beyotime, Jiangsu, China). Stained slices were observed using a laser scanning confocal microscopy.

Western Blotting

TA muscles were homogenized in cold RIPA buffer (Beyotime, Jiangsu, China) by an ultrasonic vibrator and a mechanical homogenizer. Proteins (30 mg) were separated by 10% SDS-PAGE and subsequently transferred to polyvinylidene difluoride membranes (Millipore Corp., Bedford, MA, United States). After being blocked, immunoblots were incubated with primary antibody against anti-nuclear factor erythroid-2-related factor 2 (NRF2) (1:1,000; Santa Cruz Biotechnologies), anti-p-AKT (1:1,000; ProteinTech Group, Wuhan, China), anti-AKT (1:1,000; ProteinTech Group), and anti-β-actin (1:10,000; Bioworld, Nanjing, China) at 4 °C overnight, followed by incubation with a secondary horseradish peroxidase-conjugated IgG (1:5,000; Abcam) for 1 h at room temperature. Immunoreactive proteins were visualized using the enhanced chemiluminescence Western blotting detection system (Millipore). Staining intensity of the

bands was measured using a densitometer (Syngene, Braintree, United Kingdom) together with Genesnap and Genetools software (Syngene).

Statistical Analysis

Data were presented as mean ± S.E.M. The comparison among multiple groups was performed by one-way ANOVA followed by a Bonferroni correction post-hoc test. Statistical significance was set at $p < 0.05$. All statistical analyses were done with SPSS 22.0 (SPSS Inc., Chicago, United States).

RESULTS

The Effects of Slow (GY4137) and Rapid (NaHS) H₂S Releasing Donors on Immobilization-Induced Muscle Atrophy

Muscle atrophy is characterized by muscle fibers size decrease and muscle mass loss. We first examined the effect of H₂S donor GYY4137 and NaHS on cross-sectional areas (CSAs) of skeletal muscle fibers by using H&E staining. Results of the staining showed a significant reduction of CSAs in TA muscle isolated from immobilization group mice in comparison to control group mice (**Figure 1**). Additionally, we did notice an improvement after 2 weeks of either GYY4137 or NaHS treatment (**Figures 1A–D**). We also measured the wet weights of the tibialis anterior (TA), gastrocnemius (GAS), and quadriceps (QUA) muscles. In immobilization group, the weights of skeletal muscles were significantly lower than those in control group. Both GYY4137 and NaHS treatment significantly reversed the immobilization-induced loss of skeletal muscle mass (**Figures 2A,B**).

MuRF1 and atrogin-1, two muscle-specific E3 ubiquitin ligases, are well-known to be upregulated in skeletal muscle

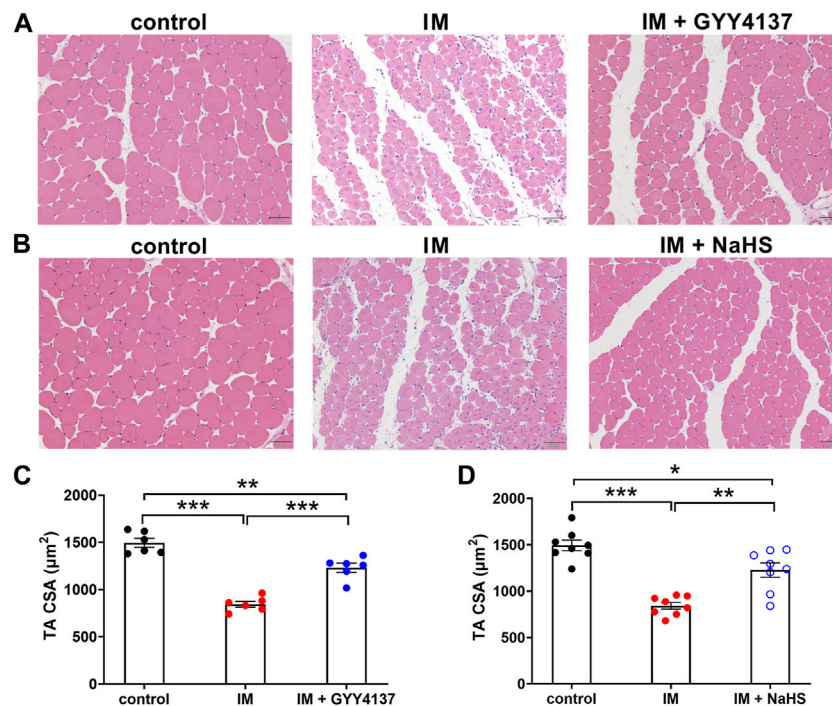


FIGURE 1 | H₂S donors alleviate the immobilization (IM)-induced muscle atrophy. Mice were subjected to IM and treated with GYY4137 (A), 50 µg/kg/d, ip, or NaHS (B), 1.12 mg/kg, twice a day, ip, for 2 weeks. The control and IM groups received identical doses of saline for 2 weeks. A & b, Representative photomicrographs of H&E-stained TA muscles (scale bars, 50 µm). (C), Quantification of fiber CSAs of TA muscle in control, IM, and IM + GYY4137 mice (n = 6 in each group). (D), Quantification of fiber CSAs of TA muscle in control, IM, and IM + NaHS mice (n = 8 in each group). Data represent means ± SEM. **p* < 0.05, ***p* < 0.01, ****p* < 0.001.

under atrophy-inducing conditions, thus serve as sensitive biomarkers related to muscle wasting. In consistent with previous studies, we found that both MuRF1 and atrogin-1 were significantly upregulated in skeletal muscles obtained from immobilization mice as compared to those obtained from control mice. Moreover, the immobilization-induced mRNA expressions of MuRF1 and atrogin-1 in skeletal muscles were significantly decreased by administration of GYY4137 and NaHS (Figures 2C,D). Taken together, these results suggesting that both slow and rapid H₂S releasing donors attenuated H₂S treatment alleviated immobilization-induced muscle atrophy.

The Effects of Slow (GYY4137) and Rapid (NaHS) H₂S Releasing Donors on Immobilization-Induced Muscle Fibrosis

Muscle fibrosis is the main cause of reduced muscle extensibility and decreased range of motion in immobilization-induced skeletal muscle atrophy. As shown in Figures 2, 3 weeks after immobilization, Masson's trichrome staining showed a significant increase in collagen deposition in the skeletal muscle. The collagen deposition appeared diffusively in the interstitium of skeletal muscle, and was accompanied by cellular infiltrates. The extensive deposition of fibrillar collagen and the destruction of normal skeletal muscle architecture observed in

immobilization-treated mice were markedly attenuated by administration of either GYY4137 or NaHS (Figures 3A–D). In addition, we also examined the mRNA expressions of tissue fibrosis biomarkers including Col1a1, Col1a2, Col5a1, Col14a1, α-SMA, PDGFRα, and TGF-β. As expected, the mRNA levels of these tissue fibrosis biomarkers were significantly increased in the immobilization group as compared to the control group. Administration of either GYY4137 or NaHS significantly inhibited the immobilization-induced mRNA expressions of Col1a1, Col1a2, Col5a1, Col14a1, α-SMA, PDGFRα, and TGF-β (Figures 4A–G). Taken together, these results indicated that both slow and rapid H₂S releasing donors attenuated immobilization-induced skeletal muscle fibrosis.

The Effects of Slow (GYY4137) and Rapid (NaHS) H₂S Releasing Donors on Immobilization-Induced Inflammatory Responses in Skeletal Muscle.

Chronic inflammatory reaction has been recognized as an important trigger of immobilization-induced muscle atrophy and fibrosis. We then investigated the effects of H₂S donor GYY4137 and NaHS on leukocyte infiltration and the mRNA expressions of the pro-inflammatory biomarkers including NLRP3, IL-1β, IL-6, TNF-α, and CCL-2 in skeletal muscles. As shown in Figure 5, there

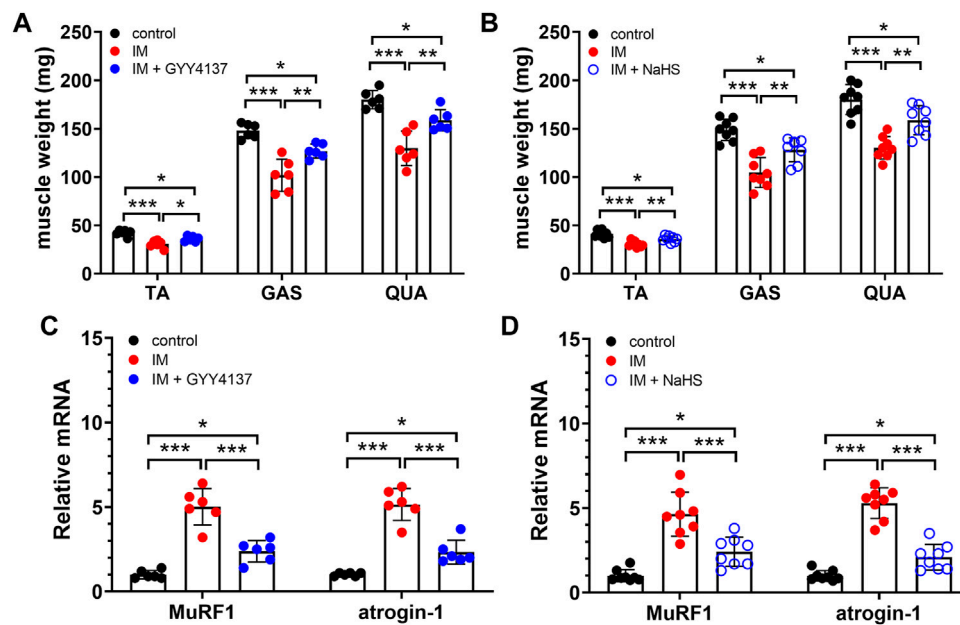


FIGURE 2 | H₂S donors protect the IM-induced muscle loss and downregulate muscle atrophy-related genes expression. Mice were subjected to IM and treated with GYY4137 (a and c, 50 µg/kg/d, ip), or NaHS (b and d, 1.12 mg/kg, twice a day, ip) for 2 weeks. The control and IM groups received identical doses of saline for 2 weeks. **(A)**, TA, GAS, and QUA muscle weights in control, IM, and IM + GYY4137 mice (n = 6 in each group). **(B)**, TA, GAS, and QUA muscle weights in control, IM, and IM + NaHS mice (n = 8 in each group). **(C)**, Expression of MuRF1 and atrogin-1 in TA muscles in control, IM, and IM + GYY4137 mice (n = 6 in each group). **(D)**, Expression of MuRF1 and atrogin-1 in TA muscles in control, IM, and IM + NaHS mice (n = 8 in each group). Data represent means ± SEM. **p* < 0.05, ***p* < 0.01, ****p* < 0.001.

were very few CD45-positive staining cells in the skeletal muscle tissues of the Control group. Mice that underwent immobilization operation developed severe infiltration of CD45⁺ leukocytes. The quantification analysis showed that the percentage of CD45⁺ leukocytes in skeletal muscles was significantly decreased by administration of either GYY4137 or NaHS (Figures 5A–D). Immobilization also caused significant increases in mRNA levels of NLRP3, IL-1β, IL-6, TNF-α, and CCL-2, which were significantly inhibited by GYY4137 or NaHS (Figures 6A–E). These data indicated that both slow and rapid H₂S releasing donors attenuated immobilization-induced inflammatory responses in skeletal muscle.

The Effects of Slow (GYY4137) and Rapid (NaHS) H₂S Releasing Donors on Immobilization-Induced Oxidative Stress in Skeletal Muscle

Oxidative stress is recently considered as another major trigger of the imbalance between protein synthesis and degradation in skeletal muscle. We then investigated the effects of H₂S donor GYY4137 and NaHS on immobilization-induced oxidative stress. As shown in Figures 7A–D, immobilization significantly increased H₂O₂ levels, whereas decreased T-AOC levels in skeletal muscles. In addition, 8-OHdG immunoreactivity, an index of oxidative DNA damage, was also profoundly increased in immobilization group as

compared with control group (Figures 8A–D). It was found that administration of either GYY4137 or NaHS significantly attenuated immobilization-induced oxidative stress as indicated by decreased H₂O₂ levels and 8-OHdG immunoreactivity, as well as increased T-AOC levels in skeletal muscles.

The Effects of Slow (GYY4137) and Rapid (NaHS) H₂S Releasing Donors on Immobilization-Induced Changes in NRF2 and NRF2 Downstream Targets in Skeletal Muscle

NRF2 has recently emerged as a potential target of associated oxidative-stress regulation (Baumfalk et al., 2021). Previous study has reported NRF2 contributed to the protective effect of H₂S against oxidative stress in a denervation induced muscle atrophy model (Kuo et al., 2015). We next examined whether NRF2 was involved in the protective effects of slow (GYY4137) and rapid (NaHS) H₂S releasing donors. In this study, we found that IM inhibited NRF2 protein and mRNA expression in TA muscle (Figure 9 and Figure 10A). Both slow (GYY4137) and rapid (NaHS) H₂S releasing donors profoundly reversed IM-induced downregulation of NRF2 protein and mRNA expression (Figures 9A–D and Figure 10A). We also measured the mRNA levels of four NRF2 downstream target anti-oxidant and cytoprotective genes, heme oxygenase-1 (HO-1), NAD(P)H dehydrogenase quinone 1 (NQO1), multidrug-resistance-associated protein 5 (MRP5), and aldo-keto reductase 1B10 (AKR1B10). As

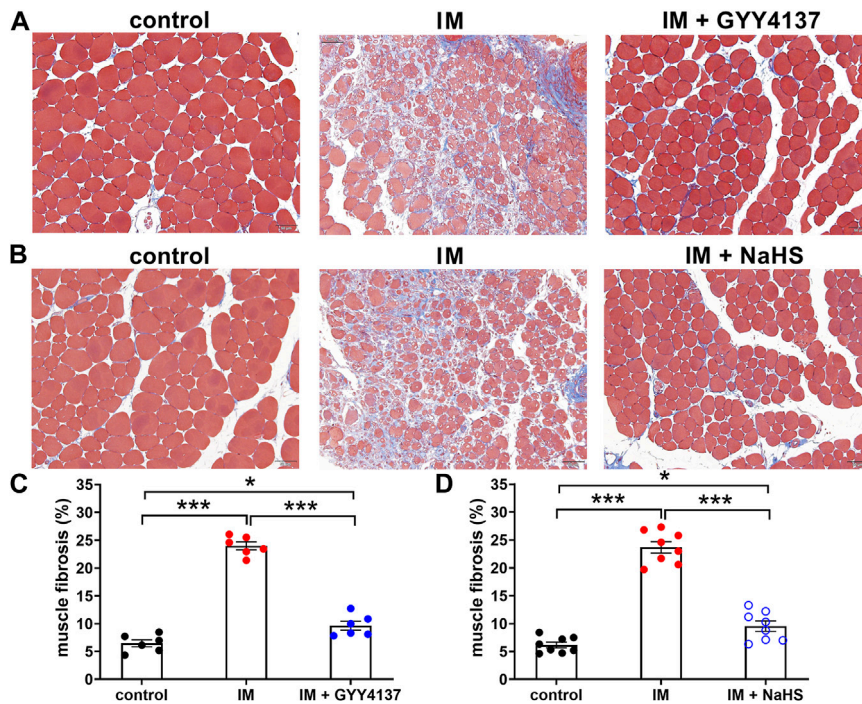


FIGURE 3 | H₂S donors reduce the IM-induced muscle fibrosis. Mice were subjected to IM and treated with GYY4137 (a and c, 50 μg/kg/d, ip), or NaHS (b and d, 1.12 mg/kg, twice a day, ip) for 2 weeks. The control and IM groups received identical doses of saline for 2 weeks. **(A)** and **(B)**, Representative photomicrographs of Masson-stained TA muscles (scale bars, 50 μm). **(C)**, Quantification of the fibrosis fraction of TA muscles in control, IM, and IM + GYY4137 mice (n = 6 in each group). **(D)**, Quantification of the fibrosis fraction of TA muscles in control, IM, and IM + NaHS mice (n = 8 in each group). Data represent means ± SEM. **p* < 0.05, ***p* < 0.01, ****p* < 0.001.

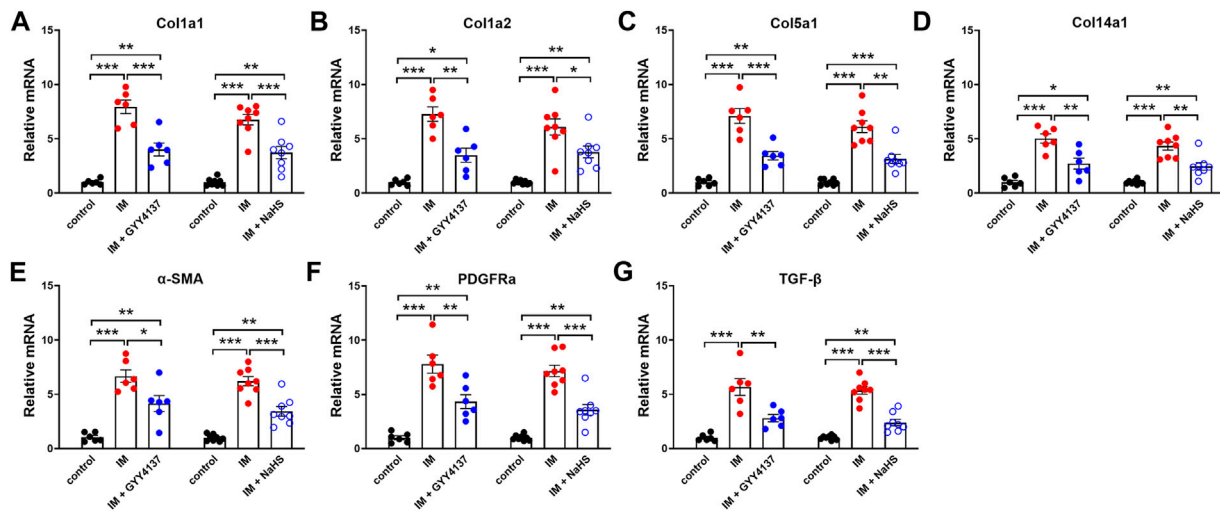


FIGURE 4 | H₂S donors downregulate the IM-induced mRNA expressions of tissue fibrosis biomarkers in skeletal muscles. Mice were subjected to IM and treated with GYY4137 (50 μg/kg/d, ip, n = 6), or NaHS (1.12 mg/kg, twice a day, ip, n = 8) for 2 weeks. The control and IM groups received identical doses of saline for 2 weeks. **(A–G)** showed mRNA expressions of tissue fibrosis biomarkers including Col1a1 **(A)**, Col1a2 **(B)**, Col5a1 **(C)**, Col14a1 **(D)**, α-SMA **(E)**, PDGFRα **(F)**, and TGF-β **(G)** in TA muscles. Data represent means ± SEM. **p* < 0.05, ***p* < 0.01, ****p* < 0.001.

shown in **Figures 10B–E**, IM led to significant decreases in HO-1, NQO1, MRP5, and AKR1B10 expression in TA muscle. Both slow (GYY4137) and rapid (NaHS) H₂S releasing donors treatments led to

significant increases in NRF2 downstream target anti-oxidant and cytoprotective genes expression compared with IM group (**Figures 10B–E**).

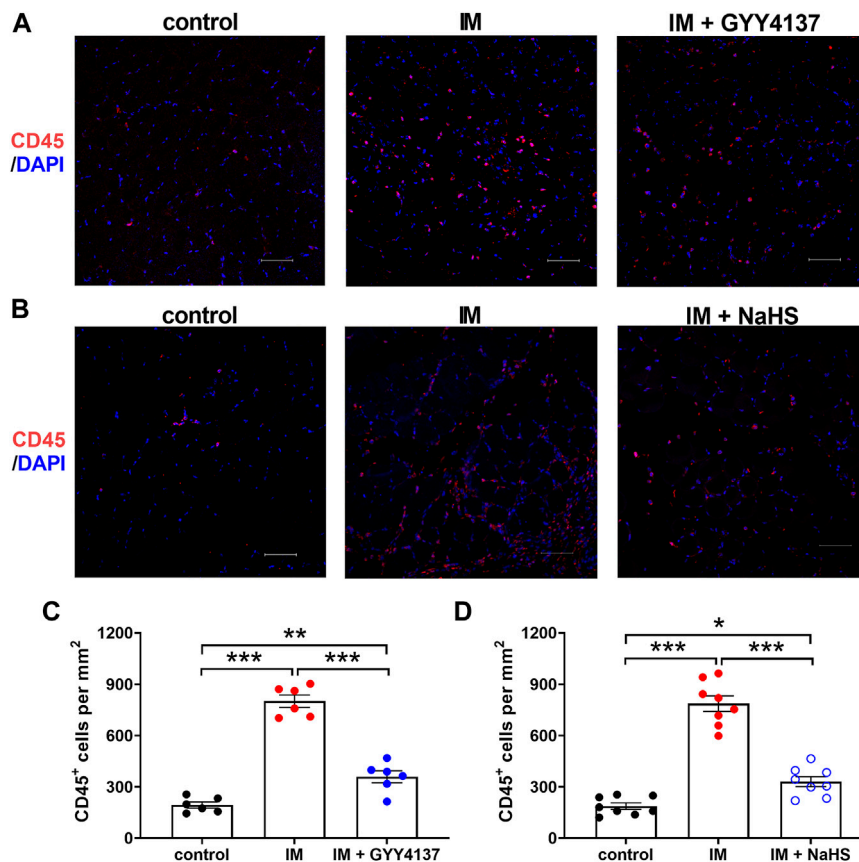


FIGURE 5 | H₂S donors alleviate the IM-induced leukocyte infiltration in skeletal muscles. Mice were subjected to IM and treated with GYY4137 (a and c, 50 μg/kg/d, ip), or NaHS (b and d, 1.12 mg/kg, twice a day, ip) for 2 weeks. The control and IM groups received identical doses of saline for 2 weeks. **(A)** and **(B)**, Representative micrographs of CD45⁺ leukocyte staining in TA muscles (Scale bar, 50 μm). **(C)**, Quantitative analysis of CD45 positive staining leukocytes of TA muscles in control, IM, and IM + GYY4137 mice (n = 6 in each group). **(D)**, Quantitative analysis of CD45 positive staining leukocytes of TA muscles in control, IM, and IM + NaHS mice (n = 8 in each group). Data represent means ± SEM. *p < 0.05, **p < 0.01, ***p < 0.001.

Either Slow (GYY4137) or Rapid (NaHS) H₂S Releasing Donors had No Significant Effect on the Expression of p-AKT/AKT Protein in Skeletal Muscle

Numerous studies have shown that H₂S can activate AKT and participate in a variety of tissue-protecting effects of H₂S (Bitar et al., 2018). We next examined whether AKT was involved in the protective effects of slow (GYY4137) and rapid (NaHS) H₂S releasing donors. In this study, we found that IM decreased p-AKT/AKT protein expression in TA muscle. However, either GYY4137 (slow releasing) or NAHS (rapid releasing) H₂S donors had no significant effect on the expression of p-AKT/AKT protein (Figure 11).

DISCUSSION

Both chronic inflammatory reaction and oxidative stress have been already proposed in the pathogenesis of skeletal muscle atrophy due to different etiologies (Moylan and Reid, 2007; Meng

and Yu, 2010). Previous studies have shown that administration of H₂S donor NaHS can alleviate skeletal muscle atrophy induced by type 2 diabetes (Bitar et al., 2018), hyperhomocysteinemia (Majumder et al., 2018), ventilator (Ichinoseki-Sekine et al., 2021), cardiotoxin (Zhang et al., 2021), and denervation (Kuo et al., 2015) by attenuating inflammation, oxidative stress and protein degradation. The present study demonstrated that treatment with either slow (GYY4137) or rapid (NaHS) H₂S releasing donors protected mice against immobilization-induced muscle atrophy. In addition, we provided several line of evidence that both GYY4137 and NaHS inhibited immobilization-induced inflammation and oxidative stress in skeletal muscles as evidenced by decreases in pro-inflammatory factors, leukocyte infiltration, H₂O₂ level, 8-OHdG immunoreactivity and increases in anti-oxidative biomarker T-AOC. These findings suggest that the inhibitory effects of H₂S on immobilization-induced inflammatory response and oxidative stress may at least partially be responsible for its protective effects against skeletal muscle atrophy.

Muscle fibrosis characterized by increased collagen deposition in the extracellular matrix is the main cause of reduced muscle

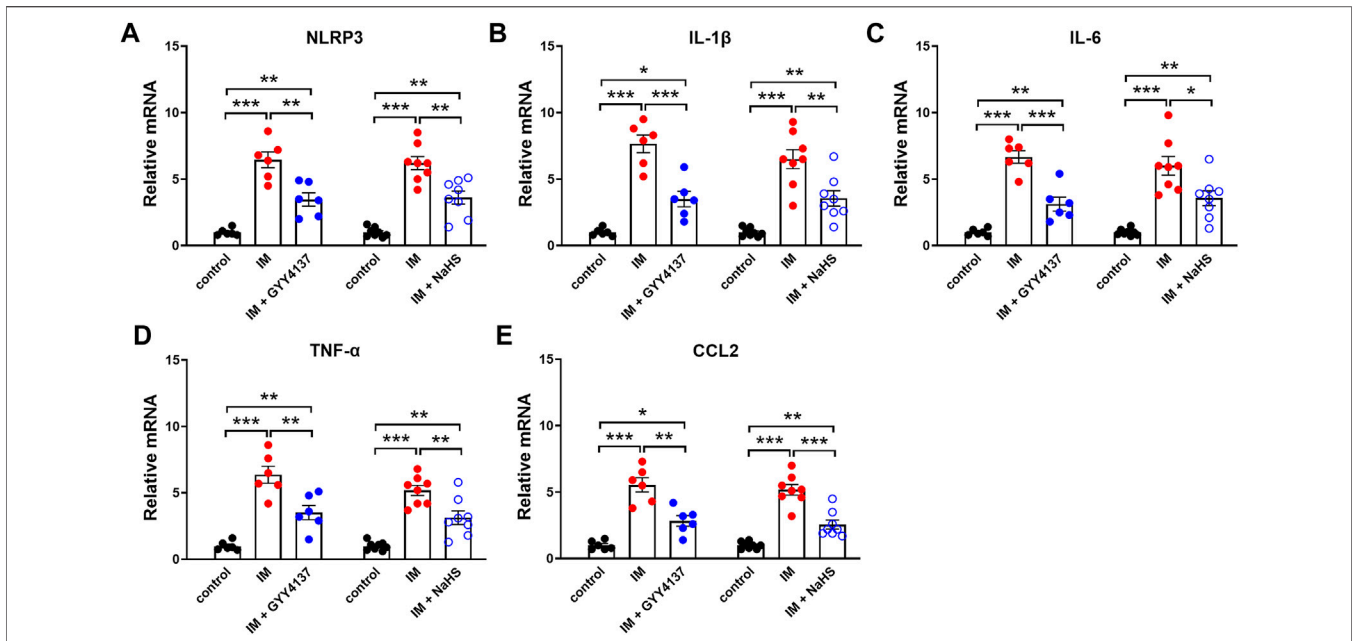


FIGURE 6 | H2S donors inhibit the IM-induced mRNA expressions of pro-inflammatory biomarkers in skeletal muscles. Mice were subjected to IM and treated with GYY4137 (50 μg/kg/d, ip, n = 6), or NaHS (1.12 mg/kg, twice a day, ip, n = 8) for 2 weeks. The control and IM groups received identical doses of saline for 2 weeks. a-e showed mRNA expressions of pro-inflammatory biomarkers including NLRP3 (A), IL-1β (B), IL-6 (C), TNF-α (D), and CCL2 (E) in TA muscles. Data represent means ± SEM. **p* < 0.05, ***p* < 0.01, ****p* < 0.001.

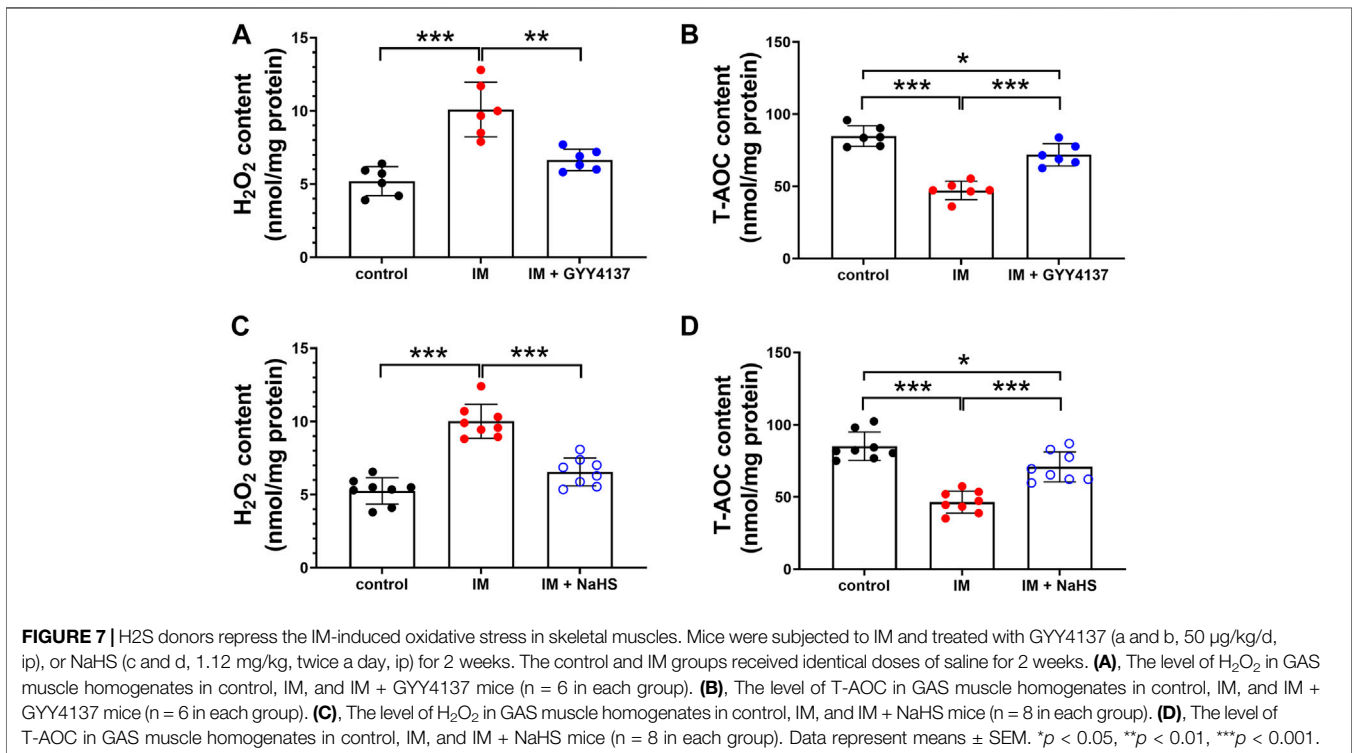


FIGURE 7 | H2S donors repress the IM-induced oxidative stress in skeletal muscles. Mice were subjected to IM and treated with GYY4137 (a and b, 50 μg/kg/d, ip), or NaHS (c and d, 1.12 mg/kg, twice a day, ip) for 2 weeks. The control and IM groups received identical doses of saline for 2 weeks. (A), The level of H₂O₂ in GAS muscle homogenates in control, IM, and IM + GYY4137 mice (n = 6 in each group). (B), The level of T-AOC in GAS muscle homogenates in control, IM, and IM + GYY4137 mice (n = 6 in each group). (C), The level of H₂O₂ in GAS muscle homogenates in control, IM, and IM + NaHS mice (n = 8 in each group). (D), The level of T-AOC in GAS muscle homogenates in control, IM, and IM + NaHS mice (n = 8 in each group). Data represent means ± SEM. **p* < 0.05, ***p* < 0.01, ****p* < 0.001.

extensibility and decreased range of motion in immobilization-induced skeletal muscle atrophy (Maezawa et al., 2017). Previous studies have shown that the accumulation of leukocytes, which

induces the differentiation of fibroblasts into myofibroblasts via IL-1β/TGF-β signaling, plays an important role during the pathogenesis of immobilization-induced muscle fibrosis

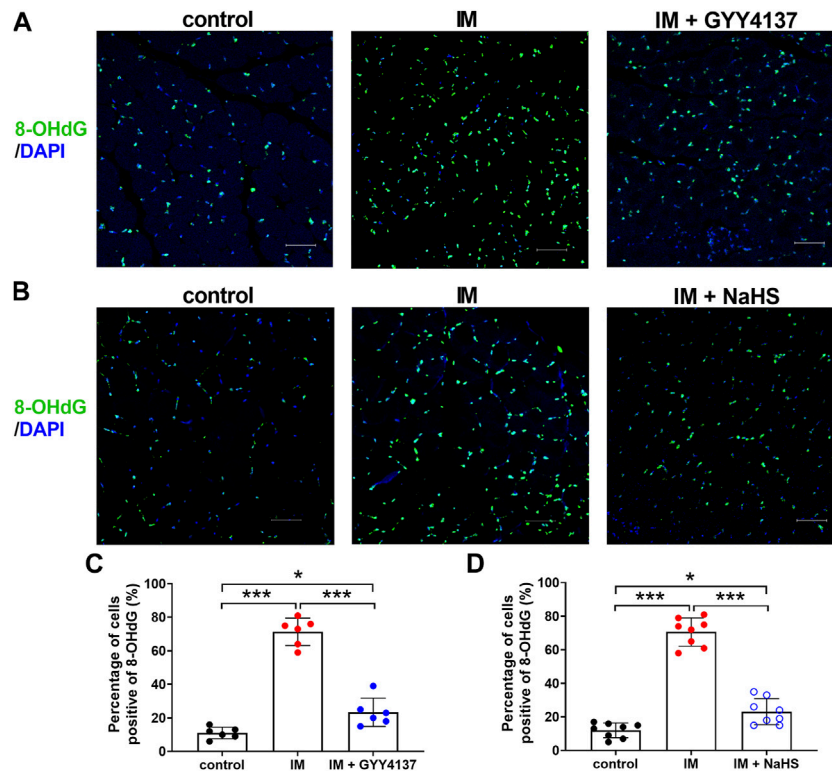


FIGURE 8 | H2S donors attenuate the IM-induced muscle 8-OHdG positive staining. Mice were subjected to IM and treated with GYY4137 (a and c, 50 µg/kg/d, ip), or NaHS (b and d, 1.12 mg/kg, twice a day, ip) for 2 weeks. The control and IM groups received identical doses of saline for 2 weeks. **(A)** and **(B)**, Representative micrographs of 8-OHdG staining in TA muscles (Scale bar, 50 µm). **(C)**, Quantitative analysis of 8-OHdG positive staining of TA muscles in control, IM, and IM + GYY4137 mice (n = 6 in each group). **(D)**, Quantitative analysis of 8-OHdG positive staining TA muscles in control, IM, and IM + NaHS mice (n = 8 in each group). Data represent means ± SEM. **p* < 0.05, ***p* < 0.01, ****p* < 0.001.

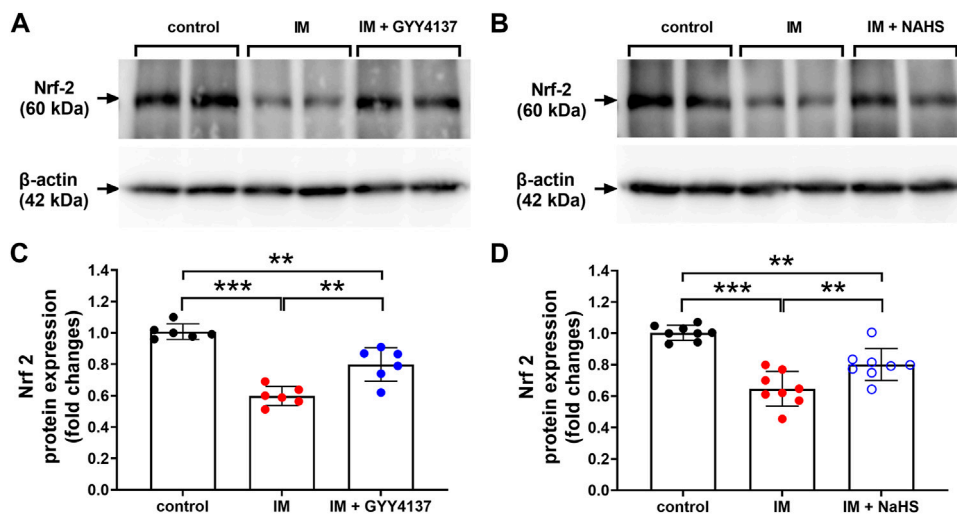
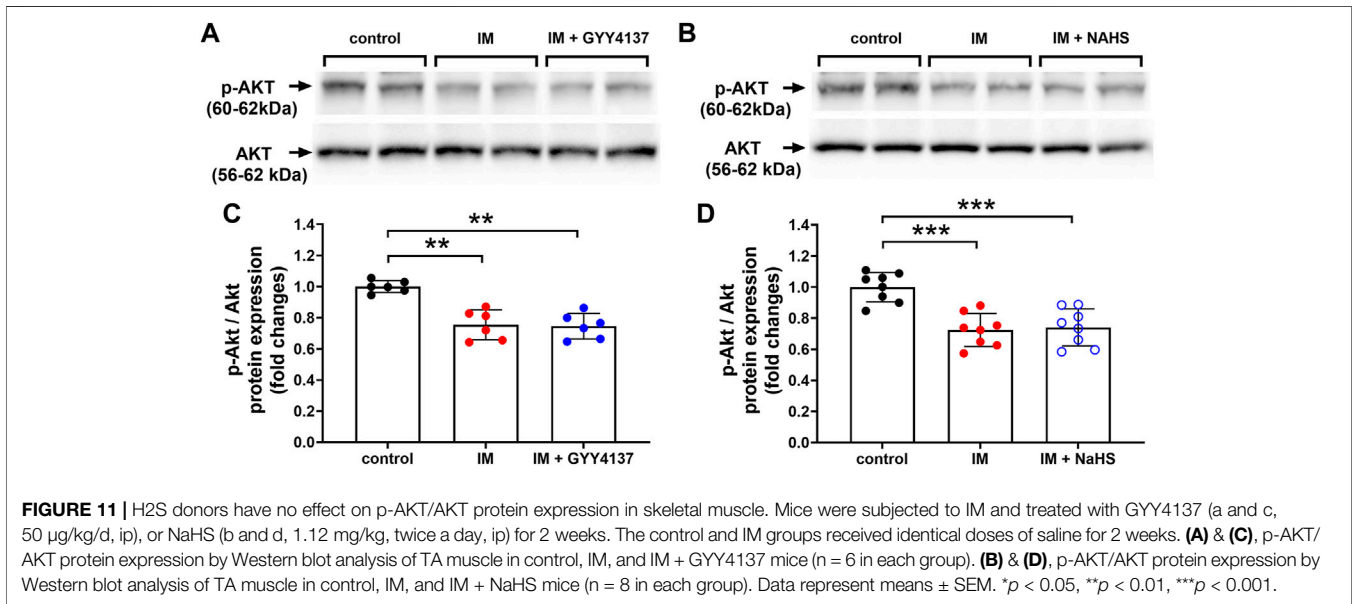
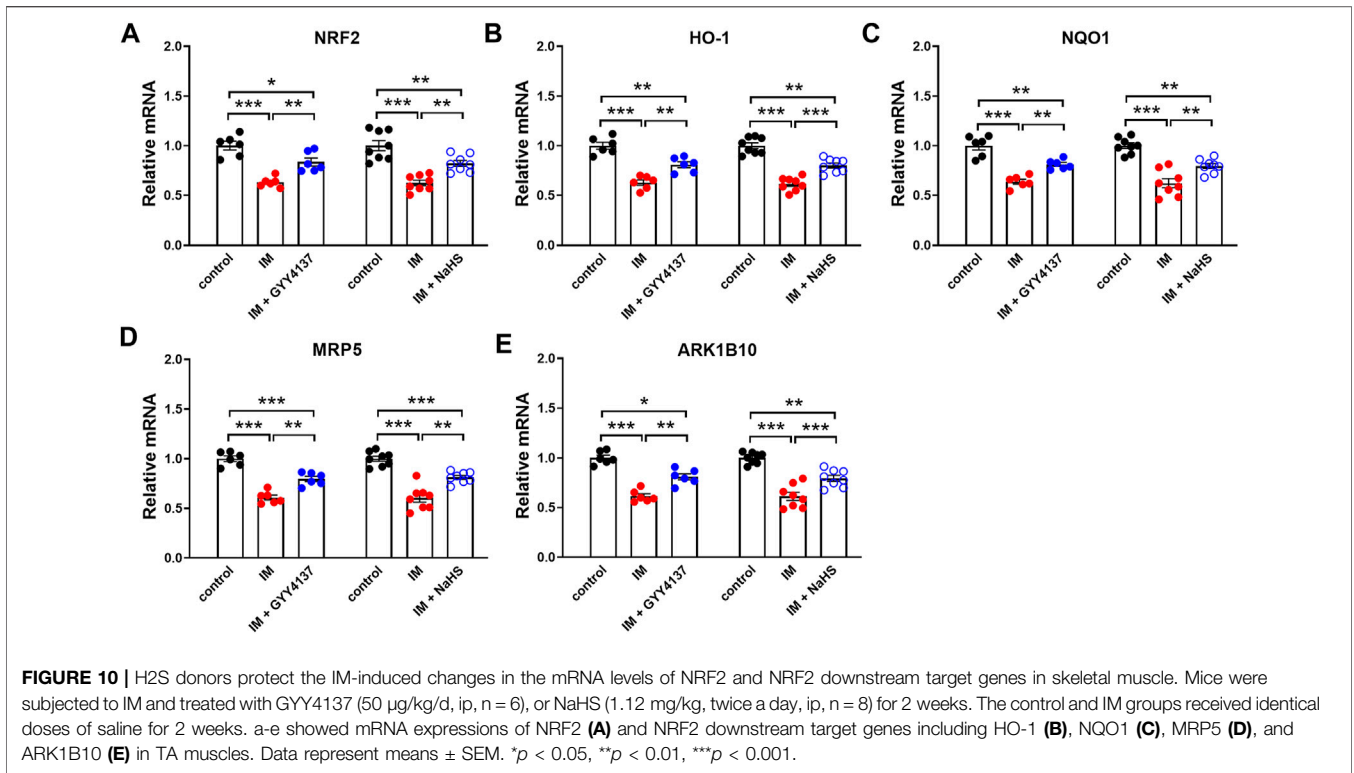


FIGURE 9 | H2S donors improve the IM-induced changes in NRF2 protein expression in skeletal muscle. Mice were subjected to IM and treated with GYY4137 (a and c, 50 µg/kg/d, ip), or NaHS (b and d, 1.12 mg/kg, twice a day, ip) for 2 weeks. The control and IM groups received identical doses of saline for 2 weeks. **(A)** & **(C)**, NRF2 protein expression by Western blot analysis of TA muscle in control, IM, and IM + GYY4137 mice (n = 6 in each group). **(B)** & **(D)**, NRF2 protein expression by Western blot analysis of TA muscle in control, IM, and IM + NaHS mice (n = 8 in each group). Data represent means ± SEM. **p* < 0.05, ***p* < 0.01, ****p* < 0.001.



(Honda et al., 2015). On the other hand, reactive oxygen species (ROS) has been shown to mediate TGF-β1-induced fibroblast activation and myofibroblast differentiation in various tissues (Cucoranu et al., 2005; Tsubouchi et al., 2017). Our previous study has found that H₂S alleviates renal injury and fibrosis in response to unilateral ureteral obstruction by attenuating macrophage infiltration (Zhou et al., 2020). In addition, H₂S

donors are also found to alleviate bleomycin-induced lung fibrosis (Du et al., 2019), transverse aortic constriction-induced myocardial fibrosis (Liu et al., 2021) and blunt contusion-induced skeletal muscle fibrosis (Zhao L et al., 2020) by attenuating oxidative stress. Consistent with these findings, the present study found that both GYY4137 and NaHS significantly decreased immobilization-induced

leukocyte infiltration and oxidative stress, reduced the production of IL-1 β and TGF- β in skeletal muscles, thus alleviating immobilization-induced muscle fibrosis.

H₂S donors have been found to exert either pro-inflammatory or anti-inflammatory effects. This discrepancy is at least partially due to the concentration and releasing rate of different H₂S donors (Bhatia et al., 2006). GYY4137 releases H₂S slowly over a period of hours, thus maintaining a stable and sustained H₂S concentration after injection *in vivo* (Li et al., 2009). In contrast, NaHS gives a rapid bolus of H₂S in aqueous solutions (De Preter et al., 2016). Whiteman et al. have compared the effects of GYY4137 and NaHS on the release of inflammatory mediators in macrophages in the same concentration range (Whiteman et al., 2010). GYY4137 concentration-dependently inhibits LPS-induced release of proinflammatory mediators, whereas NaHS elicits a biphasic effect on macrophages and, at high concentrations, increases the synthesis of proinflammatory cytokines (Whiteman et al., 2010). Similar results are documented in *in vivo* studies. GYY4137 at a dose of 50 mg/kg exerts anti-inflammatory effects in animal models of endotoxic shock (Li et al., 2009), joint inflammation (Li et al., 2013) and experimental necrotizing enterocolitis (Drucker et al., 2019). Administration of NaHS at high dose of 10 mg/kg has been shown to induce lung inflammation by itself, and also to worsen CLP-induced lung inflammation (Zhang et al., 2006). However, administration of NaHS at low dose of 0.5–2 mg/kg exerts anti-inflammatory effects in animal models of ovalbumin-induced airway inflammation (Benetti et al., 2013), homocysteine-induced neuro-inflammatory conditions (Kumar and Sandhir, 2019) and blunt contusion-induced skeletal muscle atrophy (Zhao L et al., 2020). In consistent with these studies, our findings showed that both GYY4137 (50 mg/kg) and NaHS (20 μ M/kg or 1.12 mg/kg) significantly inhibited immobilization-induced inflammation in skeletal muscles.

Skeletal muscle atrophy occurs as the result of an imbalance between anabolic and catabolic processes (Wall et al., 2013a). In a variety of muscle-wasting conditions such as cancer, diabetes, sepsis, starvation and disuse, a primary driver of muscle atrophy is thought to be an increase in protein degradation via the ubiquitin–proteasome pathway (Kandarian and Jackman, 2006; Cohen et al., 2015). MuRF1 and atrogin-1 have been well-recognized as two muscle-specific E3 ubiquitin ligases that are transcriptionally increased in skeletal muscle under atrophy-inducing conditions (Komatsu et al., 2018). In the present study, we found that immobilization-induced mRNA expressions of MuRF1 and atrogin-1 in skeletal muscles were significantly decreased by administration of GYY4137 and NaHS, suggesting that H₂S treatment inhibited MuRF1 and atrogin-1 expression in the transcriptional level. Notably, H₂S can modify target proteins by S-sulfhydration at Cys residues (Lu et al., 2020), which also serves as an important signaling mechanism by H₂S. Lu et al. recently report that H₂S treatment results in MuRF1 S-sulfhydration at the site of Cys44, thus preventing the degradation of skeletal muscle and ameliorating skeletal muscle atrophy in diabetic mice (Lu et al., 2020). The possibility that H₂S-mediated post-translational modification of muscle-specific E3 ubiquitin ligases may contribute to the protective effects of H₂S against immobilization-induced muscle atrophy merits further investigation.

In addition, NRF2 is a ubiquitous master transcription factor that regulates antioxidant response element (ARE)-mediated expression of over 200 antioxidant enzymes and cytoprotective proteins (He et al., 2020). Kelch-like ECH-associated protein 1 (Keap1) acts as a negative regulator of NRF2. H₂S has been reported to S-sulfhydrated Keap1 at cysteine-151 and induced NRF2 dissociation from Keap1, thus enhancing NRF2 nuclear translocation and transactivating the target genes of NRF2 (Yang et al., 2013). NRF2 signal is found to be down-regulated in denervation-induced skeletal muscle atrophy (Kuo et al., 2015). Baumfalk et al. have reported that NRF2 contributes to the protective effect of H₂S against oxidative stress in a prostate cancer-induced cardiac atrophy model (Baumfalk et al., 2021). Consistent with these studies, the present study demonstrated significant decreases in NRF2 expression and transcriptional levels of NRF2 downstream target genes in IM-induced atrophied skeletal muscle. Furthermore, both slow (GYY4137) and rapid (NaHS) H₂S releasing donors profoundly reversed IM-induced downregulation of NRF2 and its downstream antioxidant target genes in skeletal muscle. These findings suggest that H₂S may protect against immobilization-induced skeletal muscle atrophy, at least partly, by activating NRF2 signaling pathway.

Meanwhile, AKT regulates both protein synthesis and degradation, respectively, via the kinases mammalian target of rapamycin (mTOR) and the transcription factors of the FoxO family (Bonaldo and Sandri, 2013). On one hand, AKT enhances protein synthesis of skeletal muscle by activating AKT/mTOR and downstream signaling molecules as reflected by the phosphorylation of S6 ribosomal protein (S6) and eIF4E-binding protein (4E-BP1) (You et al., 2015). On the other hand, AKT promotes the phosphorylation of FoxO1 and consequently decreases the expression of two degradation-associated proteins, namely, MuRF1 and atrogin-1 (Sandri et al., 2004). Bitar et al. have revealed that rat diabetic atrophied muscles exhibit a state of depressed AKT activation. H₂S therapy increases AKT activity and levels of myostatin in diabetic skeletal muscle (Bitar et al., 2018). Similarly, we found that immobilization decreased phosphorylated AKT levels in TA muscles. However, either GYY4137 or NaHS had no significant effect on AKT phosphorylation in TA muscles exposed to immobilization. The discrepancy between our finding and those of Bitar et al. may be attributed to a lot of factors, such as muscle atrophy model differences and species and genus diversity of laboratory animals, which should be further investigated in the future research.

CONCLUSION

The present study demonstrated for the first time that treatment with either slow (GYY4137) or rapid (NaHS) H₂S releasing donors protected mice against immobilization-induced muscle fibrosis and atrophy. In addition, both GYY4137 and NaHS inhibited immobilization-induced inflammation and oxidative stress in skeletal muscles. These findings suggest that the beneficial effects of H₂S on immobilization-induced skeletal muscle atrophy may be

due to both the anti-inflammatory and anti-oxidant properties of H₂S, thus supporting the therapeutic potentials of H₂S donors in patients with disuse-associated muscle atrophy.

DATA AVAILABILITY STATEMENT

The raw data supporting the conclusions of this article will be made available by the authors, without undue reservation.

ETHICS STATEMENT

The animal study was reviewed and approved by The study was approved by the Ethics Review Committee for Animal Experimentation of the Shanghai University of Sport, Shanghai, China (reference number 102772019DW008).

AUTHOR CONTRIBUTIONS

JL and YL designed research; MX and XL performed research, analyzed data, and wrote the manuscript; PB and YW performed

animal experiment. All authors contributed to the article and approved the submitted version.

FUNDING

The study was supported by grants from the National Natural Science Foundation of China (Grant No. 31971102) to JL, and the National Natural Science Foundation of China (Grant No. 81672266) to YL. The study was also supported by Shanghai Frontiers Science Research Base of Exercise and Metabolic Health.

ACKNOWLEDGMENTS

The authors would like to thank all the help hands involved in this study.

SUPPLEMENTARY MATERIAL

The Supplementary Material for this article can be found online at: <https://www.frontiersin.org/articles/10.3389/fphys.2022.844539/full#supplementary-material>

REFERENCES

- Baumfalk, D. R., Opoku-Acheampong, A. B., Caldwell, J. T., Butenas, A. L. E., Horn, A. G., Kunkel, O. N., et al. (2021). Effects of High-Intensity Training on Prostate Cancer-Induced Cardiac Atrophy. *Am. J. Transl. Res.* 13 (1), 197–209.
- Benetti, L. R., Campos, D., Gurgueira, S. A., Vercesi, A. E., Guedes, C. E. V., Santos, K. L., et al. (2013). Hydrogen Sulfide Inhibits Oxidative Stress in Lungs from Allergic Mice *In Vivo*. *Eur. J. Pharmacol.* 698 (1–3), 463–469. doi:10.1016/j.ejphar.2012.11.025
- Bhatia, M., Zhi, L., Zhang, H., Ng, S.-W., and Moore, P. K. (2006). Role of Substance P in Hydrogen Sulfide-Induced Pulmonary Inflammation in Mice. *Am. J. Physiol. Lung Cell Mol. Physiol.* 291 (5), L896–L904. doi:10.1152/ajplung.00053.2006
- Bitar, M. S., Nader, J., Al-Ali, W., Al Madhoun, A., Arefanian, H., and Al-Mulla, F. (2018). Hydrogen Sulfide Donor NaHS Improves Metabolism and Reduces Muscle Atrophy in Type 2 Diabetes: Implication for Understanding Sarcopenic Pathophysiology. *Oxid. Med. Cell Longev.* 2018, 1–17. doi:10.1155/2018/6825452
- Bonaldo, P., and Sandri, M. (2013). Cellular and Molecular Mechanisms of Muscle Atrophy. *Dis. Model. Mech.* 6 (1), 25–39. doi:10.1242/dmm.010389
- Caron, A. Z., Haroun, S., Leblanc, É., Trensz, F., Guindi, C., Amrani, A., et al. (2011). The Proteasome Inhibitor MG132 Reduces Immobilization-Induced Skeletal Muscle Atrophy in Mice. *BMC Musculoskelet. Disord.* 12, 185. doi:10.1186/1471-2474-12-185
- Chen, Y., Yuan, S., Cao, Y., Kong, G., Jiang, F., Li, Y., et al. (2021). Gasotransmitters: Potential Therapeutic Molecules of Fibrotic Diseases. *Oxid. Med. Cell Longev.* 2021, 1–18. doi:10.1155/2021/3206982
- Cohen, S., Nathan, J. A., and Goldberg, A. L. (2015). Muscle Wasting in Disease: Molecular Mechanisms and Promising Therapies. *Nat. Rev. Drug Discov.* 14 (1), 58–74. doi:10.1038/nrd4467
- Cucoranu, I., Clempus, R., Dikalova, A., Phelan, P. J., Ariyan, S., Dikalov, S., et al. (2005). NAD(P)H Oxidase 4 Mediates Transforming Growth Factor- β 1-Induced Differentiation of Cardiac Fibroblasts into Myofibroblasts. *Circ. Res.* 97 (9), 900–907. doi:10.1161/01.RES.0000187457.24338.3D
- De Preter, G., Deriemaeker, C., Danhier, P., Brisson, L., Cao Pham, T. T., Grégoire, V., et al. (2016). A Fast Hydrogen Sulfide-Releasing Donor Increases the Tumor Response to Radiotherapy. *Mol. Cancer Ther.* 15 (1), 154–161. doi:10.1158/1535-7163.MCT-15-0691-T
- Drucker, N. A., Jensen, A. R., Te Winkel, J. P., and Markel, T. A. (2019). Hydrogen Sulfide Donor GYY4137 Acts through Endothelial Nitric Oxide to Protect Intestine in Murine Models of Necrotizing Enterocolitis and Intestinal Ischemia. *J. Surg. Res.* 234, 294–302. doi:10.1016/j.jss.2018.08.048
- Du, S.-F., Wang, X.-L., Ye, C.-L., He, Z.-J., Li, D.-X., Du, B.-R., et al. (2019). Exercise Training Ameliorates Bleomycin-Induced Epithelial Mesenchymal Transition and Lung Fibrosis through Restoration of H₂S Synthesis. *Acta Physiol.* 225 (2), e13177. doi:10.1111/apha.13177
- Edwards, M. H., Dennison, E. M., Aihie Sayer, A., Fielding, R., and Cooper, C. (2015). Osteoporosis and Sarcopenia in Older Age. *Bone* 80, 126–130. doi:10.1016/j.bone.2015.04.016
- Frimel, T. N., Kapadia, F., Gaidosh, G. S., Li, Y., Walter, G. A., and Vandeborne, K. (2005). A Model of Muscle Atrophy Using Cast Immobilization in Mice. *Muscle Nerve* 32 (5), 672–674. doi:10.1002/mus.20399
- He, F., Ru, X., and Wen, T. (2020). NRF2, a Transcription Factor for Stress Response and beyond. *Int. J. Mol. Sci.* 21 (13), 4777. doi:10.3390/ijms21134777
- Honda, Y., Sakamoto, J., Nakano, J., Kataoka, H., Sasabe, R., Goto, K., et al. (2015). Upregulation of Interleukin-1 β /transforming Growth Factor- β 1 and Hypoxia Relate to Molecular Mechanisms Underlying Immobilization-Induced Muscle Contracture. *Muscle Nerve* 52 (3), 419–427. doi:10.1002/mus.24558
- Huang, Y., Wang, G., Zhou, Z., Tang, Z., Zhang, N., Zhu, X., et al. (2021). Endogenous Hydrogen Sulfide Is an Important Factor in Maintaining Arterial Oxygen Saturation. *Front. Pharmacol.* 12, 677110. doi:10.3389/fphar.2021.677110
- Ichinoseki-Sekine, N., Smuder, A. J., Morton, A. B., Hinkley, J. M., Mor Huertas, A., and Powers, S. K. (2021). Hydrogen Sulfide Donor Protects against Mechanical Ventilation-induced Atrophy and Contractile Dysfunction in the Rat Diaphragm. *Clin. Transl. Sci.* 14 (6), 2139–2145. doi:10.1111/cts.13081
- Kandarian, S. C., and Jackman, R. W. (2006). Intracellular Signaling during Skeletal Muscle Atrophy. *Muscle Nerve* 33 (2), 155–165. doi:10.1002/mus.20442
- Komatsu, R., Okazaki, T., Ebihara, S., Kobayashi, M., Tsukita, Y., Nihei, M., et al. (2018). Aspiration Pneumonia Induces Muscle Atrophy in the Respiratory, Skeletal, and Swallowing Systems. *J. Cachexia Sarcopenia Muscle* 9 (4), 643–653. doi:10.1002/jcsm.12297

- Kumar, M., and Sandhir, R. (2019). Hydrogen Sulfide Suppresses Homocysteine-Induced Glial Activation and Inflammatory Response. *Nitric Oxide* 90, 15–28. doi:10.1016/j.niox.2019.05.008
- Kuo, Y.-T., Shih, P.-H., Kao, S.-H., Yeh, G.-C., and Lee, H.-M. (2015). Pyrroloquinoline Quinone Resists Denervation-Induced Skeletal Muscle Atrophy by Activating PGC-1 α and Integrating Mitochondrial Electron Transport Chain Complexes. *PLoS One* 10 (12), e0143600. doi:10.1371/journal.pone.0143600
- Li, L., Salto-Tellez, M., Tan, C.-H., Whiteman, M., and Moore, P. K. (2009). GYY4137, a Novel Hydrogen Sulfide-Releasing Molecule, Protects against Endotoxic Shock in the Rat. *Free Radic. Biol. Med.* 47 (1), 103–113. doi:10.1016/j.freeradbiomed.2009.04.014
- Li, L., Fox, B., Keeble, J., Salto-Tellez, M., Winyard, P. G., Wood, M. E., et al. (2013). The Complex Effects of the Slow-Releasing Hydrogen Sulfide Donor GYY4137 in a Model of Acute Joint Inflammation and in Human Cartilage Cells. *J. Cel. Mol. Med.* 17 (3), 365–376. doi:10.1111/jcmm.12016
- Liu, L., Gong, W., Zhang, S., Shen, J., Wang, Y., Chen, Y., et al. (2021). Hydrogen Sulfide Attenuates Angiotensin II-Induced Cardiac Fibroblast Proliferation and Transverse Aortic Constriction-Induced Myocardial Fibrosis through Oxidative Stress Inhibition via Sirtuin 3. *Oxid. Med. Cell Longev.* 2021, 1–16. doi:10.1155/2021/9925771
- Lu, F., Lu, B., Zhang, L., Wen, J., Wang, M., Zhang, S., et al. (2020). Hydrogen Sulphide Ameliorating Skeletal Muscle Atrophy in Db/db Mice via Muscle RING finger 1 S-sulfhydration. *J. Cel Mol. Med.* 24 (16), 9362–9377. doi:10.1111/jcmm.15587
- Maezawa, T., Tanaka, M., Kanazashi, M., Maeshige, N., Kondo, H., Ishihara, A., et al. (2017). Astaxanthin Supplementation Attenuates Immobilization-Induced Skeletal Muscle Fibrosis via Suppression of Oxidative Stress. *J. Physiol. Sci.* 67 (5), 603–611. doi:10.1007/s12576-016-0492-x
- Majumder, A., Singh, M., Behera, J., Theilen, N. T., George, A. K., Tyagi, N., et al. (2018). Hydrogen Sulfide Alleviates Hyperhomocysteinemia-Mediated Skeletal Muscle Atrophy via Mitigation of Oxidative and Endoplasmic Reticulum Stress Injury. *Am. J. Physiol. Cell Physiol.* 315 (5), C609–C622. doi:10.1152/ajpcell.00147.2018
- Meng, S.-J., and Yu, L.-J. (2010). Oxidative Stress, Molecular Inflammation and Sarcopenia. *Int. J. Mol. Sci.* 11 (4), 1509–1526. doi:10.3390/ijms11041509
- Moylan, J. S., and Reid, M. B. (2007). Oxidative Stress, Chronic Disease, and Muscle Wasting. *Muscle Nerve* 35 (4), 411–429. doi:10.1002/mus.20743
- Pellegrino, M. A., Desaphy, J.-F., Brocca, L., Pierno, S., Camerino, D. C., and Bottinelli, R. (2011). Redox Homeostasis, Oxidative Stress and Disuse Muscle Atrophy. *J. Physiol.* 589 (Pt 9), 2147–2160. doi:10.1113/jphysiol.2010.203232
- Sandri, M., Sandri, C., Gilbert, A., Skurk, C., Calabria, E., Picard, A., et al. (2004). Foxo Transcription Factors Induce the Atrophy-Related Ubiquitin Ligase Atrogin-1 and Cause Skeletal Muscle Atrophy. *Cell* 117 (3), 399–412. doi:10.1016/s0092-8674(04)00400-3
- Sente, T., Van Berendoncks, A. M., Franssen, E., Vrints, C. J., and Hoymans, V. Y. (2016). Tumor Necrosis Factor- α Impairs Adiponectin Signalling, Mitochondrial Biogenesis, and Myogenesis in Primary Human Myotubes Cultures. *Am. J. Physiol. Heart Circulatory Physiol.* 310 (9), H1164–H1175. doi:10.1152/ajpheart.00831.2015
- Shenton, D., Smirnova, J. B., Selley, J. N., Carroll, K., Hubbard, S. J., Pavitt, G. D., et al. (2006). Global Translational Responses to Oxidative Stress Impact upon Multiple Levels of Protein Synthesis. *J. Biol. Chem.* 281 (39), 29011–29021. doi:10.1074/jbc.M601545200
- Smink, A. M., Najdahmadi, A., Alexander, M., Li, S., Rodriguez, S., van Goor, H., et al. (2020). The Effect of a Fast-Releasing Hydrogen Sulfide Donor on Vascularization of Subcutaneous Scaffolds in Immunocompetent and Immunocompromised Mice. *Biomolecules* 10 (5), 722. doi:10.3390/biom10050722
- Tsubouchi, K., Araya, J., Minagawa, S., Hara, H., Ichikawa, A., Saito, N., et al. (2017). Azithromycin Attenuates Myofibroblast Differentiation and Lung Fibrosis Development through Proteasomal Degradation of NOX4. *Autophagy* 13 (8), 1420–1434. doi:10.1080/15548627.2017.1328348
- Wall, B. T., Dirks, M. L., and van Loon, L. J. C. (2013a). Skeletal Muscle Atrophy during Short-Term Disuse: Implications for Age-Related Sarcopenia. *Ageing Res. Rev.* 12 (4), 898–906. doi:10.1016/j.arr.2013.07.003
- Wall, B. T., Snijders, T., Senden, J. M. G., Ottenbros, C. L. P., Gijzen, A. P., Verdijk, L. B., et al. (2013b). Disuse Impairs the Muscle Protein Synthetic Response to Protein Ingestion in Healthy Men. *J. Clin. Endocrinol. Metab.* 98 (12), 4872–4881. doi:10.1210/jc.2013-2098
- Whiteman, M., Li, L., Rose, P., Tan, C.-H., Parkinson, D. B., and Moore, P. K. (2010). The Effect of Hydrogen Sulfide Donors on Lipopolysaccharide-Induced Formation of Inflammatory Mediators in Macrophages. *Antioxid. Redox Signal.* 12 (10), 1147–1154. doi:10.1089/ars.2009.2899
- Yang, G., Zhao, K., Ju, Y., Mani, S., Cao, Q., Puukila, S., et al. (2013). Hydrogen Sulfide Protects against Cellular Senescence via S-Sulfhydration of Keap1 and Activation of Nrf2. *Antioxid. Redox Signal.* 18 (15), 1906–1919. doi:10.1089/ars.2012.4645
- You, J.-S., Anderson, G. B., Dooley, M. S., and Hornberger, T. A. (2015). The Role of mTOR Signaling in the Regulation of Protein Synthesis and Muscle Mass during Immobilization in Mice. *Dis. Model. Mech.* 8 (9), 1059–1069. doi:10.1242/dmm.019414
- Zhang, H., Zhi, L., Moore, P. K., and Bhatia, M. (2006). Role of Hydrogen Sulfide in Cecal Ligation and Puncture-Induced Sepsis in the Mouse. *Am. J. Physiol. Lung Cell Mol. Physiol.* 290 (6), L1193–L1201. doi:10.1152/ajplung.00489.2005
- Zhang, Y., Masters, L., Wang, Y., Wu, L., Pei, Y., Guo, B., et al. (2021). Cystathionine Gamma-lyase/H 2 S Signaling Facilitates Myogenesis under Aging and Injury Condition. *FASEB J.* 35 (5), e21511. doi:10.1096/fj.202002675R
- Zhao L, L., Liu, X., Zhang, J., Dong, G., Xiao, W., and Xu, X. (2020). Hydrogen Sulfide Alleviates Skeletal Muscle Fibrosis via Attenuating Inflammation and Oxidative Stress. *Front. Physiol.* 11, 533690. doi:10.3389/fphys.2020.533690
- Zhao S, S., Chen, F., Yin, Q., Wang, D., Han, W., and Zhang, Y. (2020). Reactive Oxygen Species Interact with NLRP3 Inflammasomes and Are Involved in the Inflammation of Sepsis: From Mechanism to Treatment of Progression. *Front. Physiol.* 11, 571810. doi:10.3389/fphys.2020.571810
- Zhou, Y., Zhu, X., Wang, X., Peng, Y., Du, J., Yin, H., et al. (2020). H2S Alleviates Renal Injury and Fibrosis in Response to Unilateral Ureteral Obstruction by Regulating Macrophage Infiltration via Inhibition of NLRP3 Signaling. *Exp. Cel Res.* 387 (1), 111779. doi:10.1016/j.yexcr.2019.111779

Conflict of Interest: The authors declare that the research was conducted in the absence of any commercial or financial relationships that could be construed as a potential conflict of interest.

Publisher's Note: All claims expressed in this article are solely those of the authors and do not necessarily represent those of their affiliated organizations, or those of the publisher, the editors and the reviewers. Any product that may be evaluated in this article, or claim that may be made by its manufacturer, is not guaranteed or endorsed by the publisher.

Copyright © 2022 Xu, Liu, Bao, Wang, Lu and Liu. This is an open-access article distributed under the terms of the Creative Commons Attribution License (CC BY). The use, distribution or reproduction in other forums is permitted, provided the original author(s) and the copyright owner(s) are credited and that the original publication in this journal is cited, in accordance with accepted academic practice. No use, distribution or reproduction is permitted which does not comply with these terms.